Chlorination of Sulfur Dioxide in a Plasma Arc Photochemical Reactor

GEORGE J. QUARDERER
and
ROBERT H. KADLEC

Department of Chemical Engineering
University of Michigan
Ann Arbor, Michigan

SCOPE

Within the last few years plasma light sources have been introduced which possess the ability to produce high intensity levels of ultraviolet light. To the chemist or the chemical engineer then, this device suggests itself as a powerful tool with which to conduct photochemical reactions possessing a low quantum yield. The primary purpose of this investigation was to study the applicability of the plasma light source as a catalytic tool with which to promote photochemical reactions of a low quantum yield. This system has been used to determine the parameters affecting the photochemical chlorination of sulfur dioxide, a photochemical reaction known to possess a low quantum yield, with details given by Quarderer (1967).

The reactor described here is of double annular design: one annulus for an optical filter fluid, the other for reaction. Both surround an argon plasma arc. The filter fluid also serves the purpose of cooling the reaction and the light source. Light intensity can be varied by controlling power to the arc.

Spectrographic measurements were made to characterize the ultraviolet radiation emitted by the plasma light source. This radiation depends on operating parameters such as arc current and is inherently wavelength-distributed. Optical filtration of the light produced is feasible and will usually be desirable.

In 1839, Regnault reported that when a flask containing a mixture of dry sulfur dioxide and chlorine was exposed to the light of the June sun, part of the mixture combined to form sulfuryl chloride. The overall reaction is represented stoichiometrically by

$$SO_2 + Cl_2 \xrightarrow{h\nu} SO_2Cl_2$$

Since Regnault's (1839, 1840) observations, a number of investigators have studied this reaction with the result that no definitive summary of the kinetic behavior of this system is available. Various undesirable effects, such as homogeneous catalysis, heterogeneous catalysis, diffusion and chain reactions, were blamed for anomalous behavior.

The reaction rate expression for the production of sulfuryl chloride is determined experimentally. Detailed and simplified data analysis, via modeling, support a reasonable mechanism for the net formation. Light characteristics, material and energy balances, and Beer's law provide the basis for the models.

CONCLUSIONS AND SIGNIFICANCE

A basis for the design of plasma arc photochemical reactors has been presented. Mass and energy balances have been adapted to this device, and their use is demonstrated in the analysis of experimental data on the chlorination of sulfur dioxide. The efficiency of this device is 20% light from electricity but may well be higher in second-generation devices. The spectrum of an argon arc plasma is significant in the ultraviolet, which represents an advance in photochemical technology. Further development to provide safe long-term operation is necessary. The undesirable portion of the arc spectrum can be eliminated by using aqueous inorganic filter solutions.

Argon flow rate to the arc is not an important operating variable, but light output depends directly and strongly on power to the arc. The device is sensitive to electrode design but is easy to operate. There are significant axial intensity variations along the arc, necessitating stepwise calculations to quantitatively describe reactions under otherwise uniform conditions.

The forward reaction proceeds in direct proportion to the light absorbed by the reactants, with a quantum yield of one. The reverse reaction is first order in SO_2Cl_2, half order in light absorbed by reactants, and negative one-half order in SO_2. Total pressure does not affect the rate, and wall effects are not important. Only the reverse rate constant has a temperature dependence.

Because this reactor can provide large quantities of high intensity ultraviolet light, processes which are not of commercial interest with conventional light sources should be re-evaluated using this radiation source. Operating difficulties were not great in this work. This reactor can be modeled using conventional physical-chemical principles, but computer calculations are necessary due to the complexity of the light absorption process. The light source can be considered a line source for purposes of analysis.

Correspondence concerning this paper should be addressed to R. H. Kadlec. G. J. Quarderer is with The Dow Chemical Company, Midland, Michigan 48226.

Part I. Reactor Performance

This is a study of a photochemical reactor consisting of a vortex-stabilized arc and an annular, triple-walled, fused silica reaction chamber. An argon arc plasma provides the light. For power inputs of 3-12 kw, the spectral output of the light source was characterized as a function of wavelength, arc-gas flow rate, power input to the arc, and position along the arc. For power inputs of 3.84 and 8.45 kw, there were, respectively, 0.314 and 0.862 einsteins emitted per hour in the 2500 to 5000Å wavelength region. Selective filter solutions of 1.5N KNO_3 and 0.05N KI were investigated. A reactor analysis is presented, based on mass and energy balances, and the geometrical properties of the system.

Only a limited amount of published information pertaining to the construction, operation, and performance of plasma light sources (vortex stabilized arc radiation sources) is presently available in the literature. Papp (1962, 1963a, 1963b) reported that a plasma light source operating at 25 kw power input with argon as the arc gas and with an arc pressure of 17 atm had a total radiant output of 7.68 kw representing a 31% efficiency in conversion of electrical power to radiant energy. Of these 7.68 kw, 2.6 kw were found in the 2000 to 4000Å wavelength range. Papp also indicated that as power inputs increased the fraction of the total radiant energy found in the ultraviolet region increased.

Anderson et al. (1965) reported on an extensive investigation of a vortex-stabilized arc radiation source. Both total radiance and spectral distribution were measured as functions of the arc current, arc length, gas pressure in the arc, arc gas flow rate, and nozzle diameter. The authors also studied the effect of using a variety of different gases as the arc gas and reported that argon had the highest total radiance.

Lengthening the arc was observed to increase electrical efficiency for an arc length of approximately 12 cm a 60% conversion of electrical energy to radiant energy was realized. This corresponded to a radiant flux of 18 kw. Anderson and co-workers (1965) substantiate Papp's observation that as power inputs to the light source increased, the fraction of energy converted to ultraviolet radiation increased faster than that of the infrared radiation.

EXPERIMENTAL APPARATUS

The experimental system used in this investigation consisted of a plasma light source, argon delivery and cooling water systems, a dye solution recirculation system, a safety interlock system, and an ultraviolet spectrographic analysis system. A schematic diagram of the experimental apparatus is presented in Figure 1.

The photochemical reaction system used in this investigation is shown schematically in Figure 2. The system consisted of a direct current, vortex stabilized arc radiation source, and an annular triple-walled fused silica reaction chamber aligned on a common axis. The system could be operated in any attitude and could be easily disassembled.

The anode surface was fabricated from copper, while a 1% thoriated tungsten rod served as the cathode tip. The main body of each of the two electrodes was constructed of brass. Each was held in position by a laminated plastic Micarta end piece which provided electrical insulation between electrodes. The length of the arc was determined by adjusting the position of the tungsten rod relative to the main body of the cathode. Separate cooling water passages were built into both of the electrodes, with metal-to-metal seals being provided by "O"-rings.

The inner wall of the annular reaction chamber was sealed to the main body of each of the electrodes of the light source by means of "O"-ring seals, forming a transparent envelope for the arc. The argon arc gas was introduced into this envelope tangential to the inside circumference of the fused silica cylinder, forming a vortex as it spun to the central axis, exhausting through a hole at the anode tip.

The vortex flow fixed the dimensions and the location of the arc. It also served to centrifuge the hotter argon atoms to the center of the column of plasma, thus keeping the inside quartz wall of the arc envelope relatively cool.

The argon for the plasma was supplied through a calibrated rotameter. As the gas exited from the anode, it was first cooled by passing it through a small heat exchanger and was then vented to the atmosphere.

Tap water was used to cool both electrodes and the arc gas heat exchanger. The tap water was supplied to the cooling channels by a positive displacement gear pump. The various cooling water flow rates were measured with calibrated rotam-

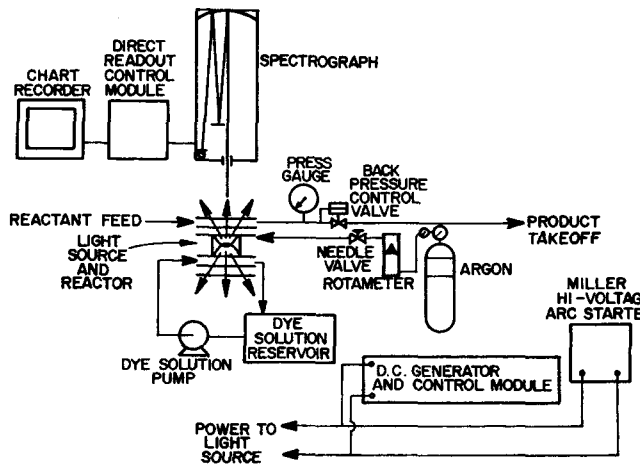

Fig. 1. Schematic diagram of experimental apparatus.

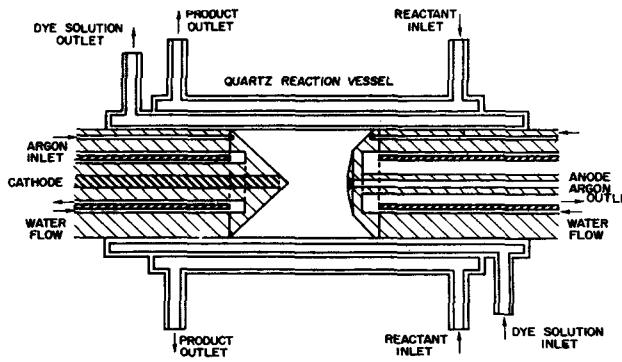

Fig. 2. Schematic diagram of photochemical reaction system.

eters. Calibrated iron-constantan thermocouples were used in all gas and water streams. The output from the various thermocouples could be switch-selected and were measured on a potentiometer.

The dc power generator was rated at 40 kw with a maximum output of 60 kw. The rated current load was 1000 A. The power unit was a three-phase transformer with three-phase full-wave bridge rectification, utilizing a saturable reactor current control device. The power supply control system also monitored the voltage and current and provided for automatic stopping of the generator in case of a loss of pressure by the cooling water or the arc gas. The plasma arc column was initiated by using a high-frequency arc starter to effect partial ionization of the arc gas.

Water soluble inorganic dyes, which provided selective wavelength filtration and cooled the inner quartz wall, were circulated through the inner of the two annular regions. The dye solution circulated through the inner annulus was either distilled water, a potassium iodide solution, or a potassium nitrate solution. The dye solution was stored in a 20-liter glass vessel and was circulated by a positive displacement gear pump. Before returning the dye solution to the storage vessel, it was cooled by heat exchange with tap water.

The outer annulus of the quartz chamber served as the actual reactor volume. Two inlets and exits were provided for the reactant gas flow in order to ensure an essentially linear flow profile as the reactant mixture traveled down the annulus.

The radiation emitted by the light source was analyzed with a 3.4-m focal length Ebert Mark IV stigmatic plane grating spectrograph. The spectrograph was equipped with a grating ruled with 15,000 lines/in. which gave a first-order linear dispersion of 5.1 Å/mm at the focal plane. The useful range of the grating was from 2100 to 7500 Å. The scanning and condensing system could scan and bring selected areas of an extended source into focus on the spectrograph slit. The system of six front surfaced mirrors and two quartz-lithium fluoride acromatic doublet lenses automatically maintained focus and alignment with the optical axis of the spectrograph. The lenses effected a 2.28 to 1 reduction in image size between the light source and the spectrographic slit. The plasma was scanned horizontally (along the plasma axis of symmetry) by turning a screw drive mechanism which moved the mirror assembly. This scan mechanism permitted accurate positioning along the plasma column.

The spectrograph was equipped with a sine bar wavelength drive which rotated the grating in a manner such that the wavelength seen by the center of the focal plane corresponded to the number recorded on a wavelength counter. The sine bar wavelength drive permitted twelve rates of scan ranging from 1 to 500 Å/minute. The spectra were recorded with a 1 P28 photomultiplier tube located at the center of the focal plane. The tube was operated with a supply voltage of 1000 vdc, monitored by a dc digital voltmeter with an absolute accuracy of ± 0.1 v. The current output of the photomultiplier tube was passed through a variable precision resistor. The resulting voltage was amplified by a variable range stabilized dc μv amplifier. The (0-10 mv) output of the amplifier was monitored with a strip chart recorder.

ANALYSIS OF SPECTROGRAPHIC MEASUREMENTS

Two light intensity units will be defined and used throughout this report. They are the spectral radiance $Q(\lambda)$ of the arc expressed in einsteins emitted per hour per Ångstrom unit of wavelength per centimeter of arc length per steradian and the spectral output of the arc expressed in einsteins emitted per hour per Ångstrom unit of wavelength per steradian. The spectral output of the arc is equal to the spectral radiance integrated over the length of the arc.

The photomultiplier tube and the optical system of the spectrograph were calibrated by spectrographically observing a luminous tungsten ribbon filament and a hydrogen lamp, standard sources whose spectral radiances were calculable. The current output of the photomultiplier tube as a function of wavelength was then compared with the calculated spectral radiance of the standard source. The ratio of the spectral radiance to the photomultiplier current output, designated by $R(\lambda)$, represents the spectral-response characteristic function for the photomultiplier tube and the optical system. This calibration factor $R(\lambda)$ had units of einsteins per hour per Ångstrom per centimeter per steradian per ampere. During calibration, the area of the source subtended by the slit was

$$S = H_c W_c / M^2 \tag{1}$$

with M being the overall image magnification effected by the lenses in the scanning and condensing system, and H_c and W_c being the slit height and slit width during calibration. The magnification factor for the lens system M was calculated by considering the spatial location of the components of the optical scanning-condensity system and the focal lengths of the two quartz-lithium fluoride acromatic doublet lenses.

During this investigation, the quantity of interest was the spectral radiance, $Q(\lambda)$, which can be expressed as

$$Q(\lambda) = \frac{R(\lambda) \cdot A(\lambda) \cdot H_c \cdot W_c}{H_I W_I} \tag{2}$$

where $A(\lambda)$ is the current output of the photomultiplier as a function of wavelength and W_I and H_I are the slit width and height used during the investigation.

PERFORMANCE CHARACTERISTICS OF THE LIGHT SOURCE

The spectral radiance $Q(\lambda)$ of the light source was determined as a function of the arc gas flow rate, position along the arc, and the power input to the arc column. For the gas flow rates investigated, spanning the entire range of stable operation, the spectral radiance varied only slightly with changing argon flow rate. Figure 3 shows the dependence of spectral radiance on argon flow rate for light having a wavelength of 3000Å and for a power input to the arc of the light source of 8.10 kw. Under these conditions a 90% increase in argon flow rate resulted in only a 2.1% increase in the 3000Å spectral radiance of the light source. During the remainder of the investigation the effect of argon flow rate on the spectral radiance was neglected. The only criterion used in select-

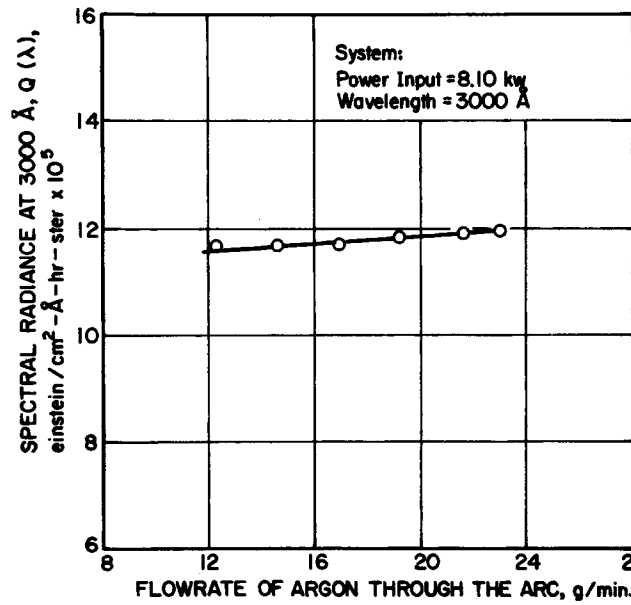

Fig. 3. Effect of argon flow rate on the spectral radiance of the arc.

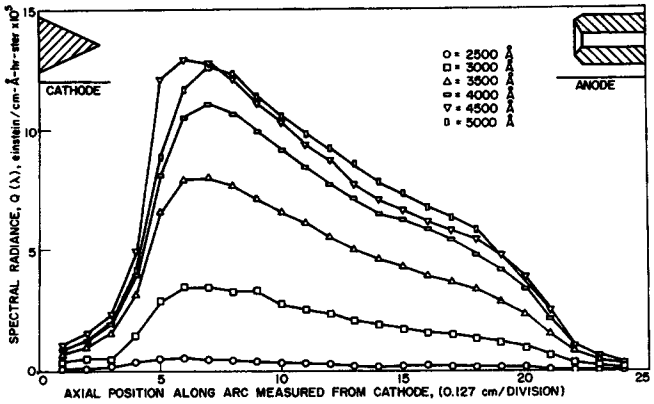

Fig. 4. Spectral radiance of the arc operating at 3.84kw vs. axial position along arc for several wavelengths.

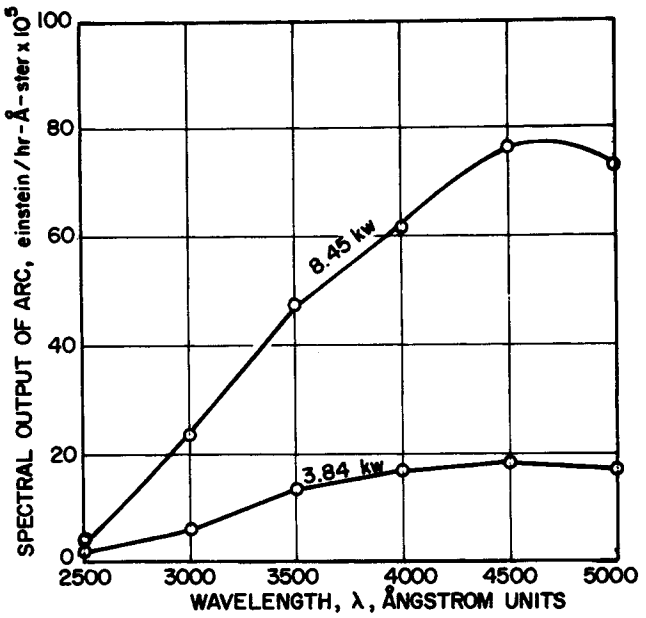

Fig. 5. Spectral output of the arc vs. wavelength for operation at power inputs of 3.84 and 8.45kw.

ing the argon flow rate was that the light source operate in a stable manner.

The spectral radiance of the light source was investigated extensively as a function of the power, wavelength, and axial position. All spectra prepared during this investigation were scanned at 100 Å/min. At this scan rate the peak heights were attenuated, but the spectral output should be unaffected. Continuum radiation was considered in calculations pertaining to the spectral output of the light source, but some radiation was in the form of line radiation. Calculated values of the available light are accurate, but there was a displacement of some line radiation. The argon line radiation was not appreciable below approximately 3450Å. However, above this wavelength it was a significant fraction of the total spectral contribution. The experimental observations are presented in Figures 4 and 5. As a matter of convenience, the arc length was subdivided into 25 regions, measuring from the vicinity of the tungsten cathode to the vicinity of the anode (see Figure 4). Each region was 0.127 cm (0.05 in.) long. The arc was observed spectrographically at the 24 points which subdivided the arc.

In Figure 5 is shown the spectral output of the light source as a function of wavelength for operation of the light source at 3.84 and 8.45 kw, respectively. Integrating under the spectral output curves with respect to wavelength, between the limits of 2500 and 5000Å, indicates that there was approximately 0.314 and 0.862 einstein/hr., respectively, of ultraviolet light available from the light source.

LINE SOURCE APPROXIMATION

Correct treatment of light intensity is the key ingredient in proper calculations. A considerable simplification in calculations can be gained by assuming that the arc column can be represented as a linear radiation source rather than an extended source. This is not always justified, as discussed by Irazoqui (1973). A partial justification for this assumption can be obtained by considering the scheme shown in Figure 6. A transparent radiating cylinder of gas having a length L and a radius R_0 is aligned on a common axis with an infinitely long second cylinder of radius R_1. The radiating cylinder is characterized by a constant value E representing the radiation-emission rate from the gas per unit of volume in all directions from a small volume element of the cylinder.

The amount of light emitted by a small volume element of the radiating gas which passes through a small area of the larger cylinder can be shown to be

$$E(\lambda)\,\frac{R_1}{4\pi}\cdot\frac{(R_1 - r\cos(\theta-\phi))\cdot r\,d\phi\,dr\,dx\,d\theta\,dz}{((x-z)^2 + R_1^2 + r^2 - 2rR_1\cos(\theta-\phi))^{3/2}} \tag{3}$$

Integrating over the various dimensions yields the total radiation passing through the outer cylinder per unit of axial length:

$$E(\lambda)\,\frac{R_1}{4\pi}\int_{-L/2}^{L/2}dx\int_0^{R_0}r\,dr\int_0^{2\pi}d\theta\int_0^{2\pi}\frac{(R_1 - r\cos(\theta-\phi))\,d\phi}{((x-z)^2 + R_1^2 + r^2 - 2rR_1\cos(\theta-\phi))^{3/2}} \tag{4}$$

A standard table of integrals permits integration of (4) over the range of the variable x, this yields

$$I(\lambda) = E(\lambda)\,\frac{R_1}{4\pi}\int_0^{R_0}r\,dr\int_0^{2\pi}d\theta\int_0^{2\pi}\frac{(R_1 - r\cos(\theta-\phi))}{(R_1^2 + r^2 - 2rR_1\cos(\theta-\phi))}\left\{\frac{(L/2+z)}{((L/2-z)^2 + R_1^2 + r^2 - 2rR_1\cos(\theta-\phi))^{1/2}} + \frac{(L/2+z)}{((L/2+z)^2 + R_1^2 + r^2 - 2rR_1\cos(\theta-\phi))^{1/2}}\right\}d\phi \tag{5}$$

Now consider a similar situation with a radiating line of length L replacing the radiating cylinder. It is assumed that the total emissions by both sources are equal, that is, $\pi R_0^2 E = Q$ is the radiation-emission rate from the source per unit of length in all directions from a small element of the line. The amount of light emitted by a linear increment of the line which passes through a small area of the outer cylinder is

$$E(\lambda)\,\pi R_0^2\,\frac{R_1^2\,d\theta\,dz\,dx}{4\pi((x-z)^2 + R_1^2)^{3/2}} \tag{6}$$

Integrating over the x and θ dependencies yields the total radiation passing through the outer cylinder per unit

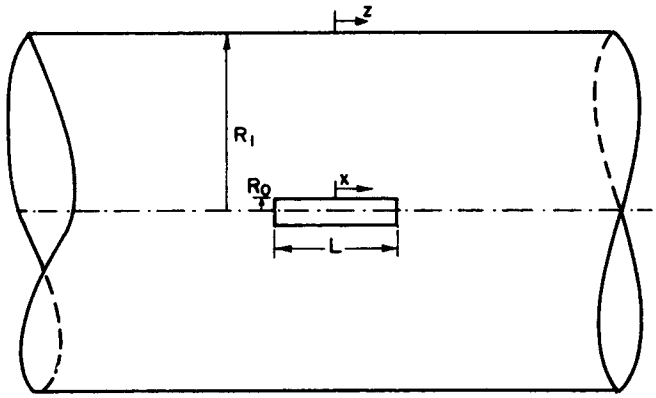

Fig. 6. Schematic diagram of an extended radiation source.

of axial length

$$I'(\lambda) = \frac{E(\lambda)\,\pi R_0^2}{2}\left(\frac{(L/2-z)}{((L/2-z)^2+R_1^2)^{1/2}} + \frac{(L/2+z)}{((L/2+z)^2+R_1^2)^{1/2}}\right) \quad (7)$$

The values of the quantities $I(\lambda)$ and $I'(\lambda)$ can now be compared. If it can be shown that the integrand of (4) is only a weak function of r and $(\theta - \phi)$, that is, is only a function of R_1, it can readily be seen that the light distribution resulting from the line source assumption is exactly that resulting from the more rigorous assumption of an extended source.

In order to investigate these dependencies, the following parameter values, characteristic of the light source used in this investigation, were used:

$$R_0 = 0.15 \text{ cm}$$
$$L = 2.41 \text{ cm} \quad (8)$$
$$R_1 = 3.63 \text{ cm}$$

Numerical investigation indicated that the integrand varied by less than ± 3% from the line source approximation for arbitrary points in the plane. For the values of the parameters indicated in (8), the error involved in equating I' with I is less than 1%.

THEORETICAL REACTOR ANALYSIS

Several excellent papers concerning modeling of photoreactors have appeared in the literature in the last few years. The reader is referred in particular to the work of Ragonese and Williams (1971) and to the critical review of Cassano et al. (1967). Applications have been given, for example, by Sandru and Smith (1973) and Matsuura and Smith (1970). The following is a similar development adapted to the plasma arc photochemical reactor.

It is possible to analyze the operation of this reactor system for purposes of design or analysis. In either case, the objective is to obtain a realistic mathematical model for the operation of this variety of reactor. In the absence of catalytic effects (wall catalysis is not uncommon), the reaction rate may be presumed to depend upon composition, temperature, and the amount of light absorbed by the various components:

$$r = f(J_i, Y_i, T) \quad (9)$$

In addition, one must know the overall stoichiometry involved, which for a single reaction may be written as follows:

$$\sum_i^{h\nu} a_i A_i = 0 \quad (10)$$

If the reactor is operated at very low throughputs, that is, in laminar flow, a complete description would involve the simultaneous solution of differential energy, mass, and momentum balances. Such a model would be quite intractable due to the extreme complexity and the lack of information about parameters such as multicomponent diffusivities. Consequently, we begin with the assumption that the reactor will be operated in turbulent flow or that the solution the momentum balance is known and uncomplicated. Since the reactor is axisymmetric, and since steady operation is feasible and desirable, time and one spatial dimension are removed from the problem. Under these conditions, the mass balance for the jth component is

$$D_{jr}\frac{1}{r}\frac{\partial}{\partial r}\left(r\frac{\partial C_j}{\partial r}\right) + D_{jz}\frac{\partial^2 C_j}{\partial z^2} - \frac{\partial}{\partial z}(uC_j) - r_j = 0 \quad (11)$$

In writing Equation (11), it has been assumed that constant effective diffusivities exist for component j, which may be different for the radial and axial directions. By appropriate design—namely a long, narrow annular reactor—the diffusion effects can be made negligible, resulting in the usual plug flow reactor equation:

$$\frac{\partial}{\partial z}(uC_j) = -r_j \quad (12)$$

If the stoichiometry is now used, all compositions may be expressed in terms of the fractional conversion of the limiting reactant, and only the rate of conversion of that reactant need be used:

$$F_0 Y_{l0}\frac{dX}{dz} = Ar_l \quad (13)$$

$$r_l = f_l(J_i, X, T, b_i) \quad (14)$$

This procedure introduces the feed ratios b_i, the moles of component i fed per mole of limiting reactant fed.

Coupled with this mass balance is an energy balance which includes the effects of convective heat transfer, light absorption, and heat of reaction:

$$-F_0 Y_{l0}\frac{d}{dz}\left\{\sum_i\left(b_i - \frac{a_i}{a_l}\right)\int_{T_R}^{T} c_{pi}dT\right\} + (-\Delta H_R)Ar_l + U\bar{A}(T_S - T) + A\sum_i W_i = 0 \quad (15)$$

The heat generated by the light absorbed by species i, denoted by W_i, is a function of distance in the reactor. It must be computed from a knowledge of the intensity and spectral distribution of the light incident at a given location, and the absorptive properties of component i. The preceding section demonstrated how the radiation arriving per unit length per unit wavelength $I(\lambda)$ could be computed from the spectral radiance $Q(\lambda)$ a measurable quantity. Beer's law provides the necessary link between incident and absorbed light (small curvature, thin annulus):

$$J_j(\lambda) = \frac{\epsilon_j(\lambda)C_j(z)}{\sum_{j=1}^{N} \epsilon_j(\lambda)C_j(z)} \left[1 - 2.303 \exp \left[\sum_{j=1}^{N} \epsilon_j(\lambda)C_j(z)d \right] \right]$$

$$\cdot I(\lambda) = \psi(\lambda, x, z)I(\lambda) \quad (16)$$

Thus, a complex situation still remains: the amount of light absorbed depends upon the absorbing species, both its concentration and molecular extinction coefficient. Concentration is position dependent and the extinction coefficient is wavelength dependent. The path length through the reacting mixture is not a constant, but a function of the positions of both the receiving and emitting elements:

$$d(x, z) = d_0 \frac{\sqrt{(x - z)^2 + R_1^2}}{R_1} \quad (17)$$

In addition, the energy associated with this light absorption is wavelength dependent, in fact equal to $h\bar{c}/\lambda$. Combining the above relations results in the expression for W_i:

$$W_i = \int_0^{\infty} \int_0^{2\pi} \int_{-L/2}^{+L/2} \left[Q(\lambda, x) \frac{R_1^2}{4\pi[(x - z)^2 + R_1^2]^{3/2}} \right] [\psi(\lambda, x, z)] \left[\frac{h\bar{c}}{\lambda} \right] dx d\theta d\lambda \quad (18)$$

The light absorbed is given by a similar integral, with the factor $h\bar{c}/\lambda$ omitted. A calculation of the light intensity produced in the actual reactor used in this study is presented in Figure 7. A uniform distribution of line-source spectral radiance was used in this calculation.

The model of this reaction system consists of Equations (13) to (15), (17), (18) and some expression relating mole fraction to other fluid properties, for example, for a gaseous system:

$$C_i = \frac{PY_i}{RT} \quad (19)$$

Composition variables X and Y_i are of course related via the stoichiometry of the system:

$$Y_j = Y_{j0} \left\{ \frac{b_j - \frac{a_j}{a_i} X}{1 - \frac{\Sigma a_j}{a_i} X Y_{i0}} \right\} \quad (20)$$

For a given rate expression, it is possible to numerically integrate these equations over the length of the reactor. The required input information includes: b_i, a_i, T_0, T_s, $Q(\lambda, x)$, $\epsilon_i(\lambda)$, U, $(-\Delta H_R)$, F_0, Y_{i0}, c_{pi}, L, P, and R_1. Such an integration yields temperature and composition profiles in the reactor. Minor modifications are possible, such as the addition of a heat balance on the dye solution to determine $T_s(z)$.

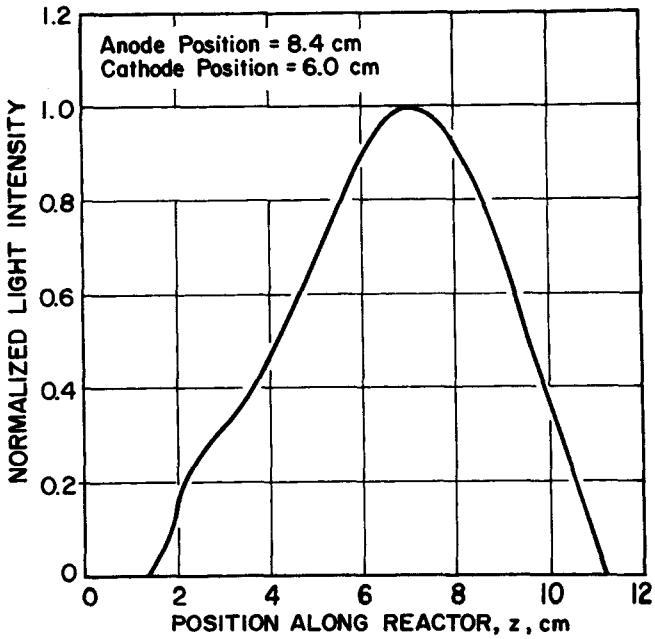

Fig. 7. Predicted variation of light intensity along the length of the reactor.

OPTICAL FILTRATION SYSTEM CHOICE

Since all photochemical reaction systems exhibit strong wavelength dependence, it is of interest to find methods for varying the wavelength distribution of the output of the light source. The obvious method of optical filtration, while easy in principle, is not easy in application. The construction of the glass reactor with a glass filter as one concentric wall is too restrictive and prohibitively expensive. The alternative is to pass a light-absorbing fluid through the inner annulus of the reactor. This serves the additional purpose of providing the necessary cooling for the arc itself.

In order to possess the desired absorption properties, a compound, or a mixture of compounds, must absorb light selectively over the wavelength region of interest. The ideal light absorbing medium would possess the following properties:

1. It would absorb strongly at wavelengths shorter than some wavelength λ_0, but would be completely transparent at wavelengths longer than λ_0.
2. λ_0 would be at a point of interest in the wavelength interval.
3. The material would not decompose photolytically when it absorbed light.
4. The compound would itself be usable as a heat transfer fluid or, alternatively, a sufficient amount of the compound could be dissolved in water.
5. The compound would not react chemically with the pump, the heat exchanger, or other items in the light filtration system.

To illustrate the problems of selecting such a filter medium, consider the specific example of the reaction between sulfur dioxide and chlorine:

$$SO_2 + Cl_2 \xrightarrow{h\nu} SO_2Cl_2$$

The light absorption properties of the reactant species are shown in Figure 8. For purposes of this example, two values of λ_0 are of interest. The lower, 2600Å, would pass nearly all light that could be absorbed by sulfur dioxide and chlorine but would filter wavelengths that would be absorbed by sulfuryl chloride. The second value of λ_0, 3300Å, would filter light that could be absorbed

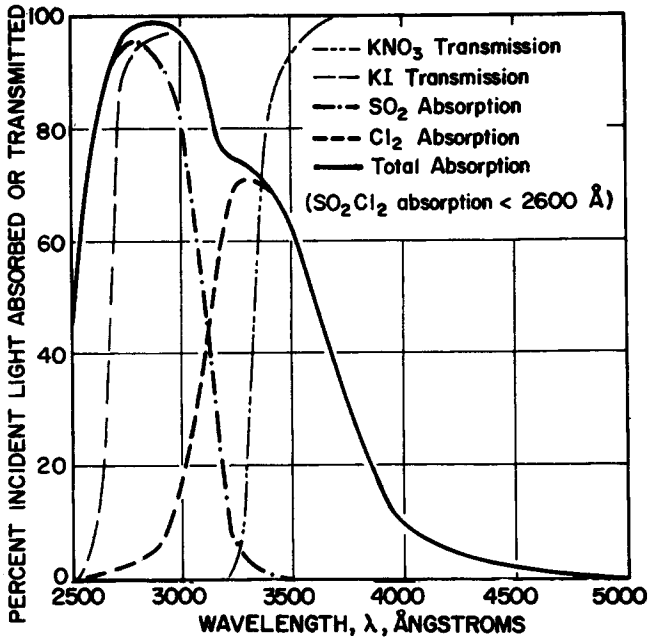

Fig. 8. Percent incident light absorbed vs. wavelength for reactants composition: ½ chlorine, ½ sulfur dioxide and transmission characteristics of 0.579 cm of 1.5N KNO_3 and 0.05N KI.

by sulfur dioxide and sulfuryl chloride, but would pass a large percentage of the light which could be absorbed by chlorine.

No single compound or group of compounds completely satisfies all of the requirements listed above. The nitrates and the iodides of the alkali metals came the closest to fulfilling all the requirements.

The percentage of incident light transmitted by 0.579 cm of a 1.5 normal aqueous solution of potassium nitrate is shown in Figure 8 as a function of the wavelength of the incident light. The cut-off region (wavelength region in which percent transmission increases from 10 to 90%) was 3260 to 3450Å. The only major drawback of the potassium nitrate solutions is that they decompose slowly as they absorb light. The photochemical decomposition of potassium nitrate has been investigated by Villars (1927). His work demonstrates that there is a strong relationship between the *p*H of the nitrate solution and the quantum yield of the photolytic reaction. Using Villars' results, the nitrate solutions used in this investigation were buffered at a *p*H of 5.0 using an acetic acid-sodium acetate mixture. This reduces the expected quantum yield for the photolytic decomposition of a value less than 0.01.

Figure 8 also shows the percentage of incident light transmitted by 0.579 cm of a 0.05 normal aqueous solution of potassium iodide as a function of the wavelengths of the incident light. Cut-off occurs between 2600 and 2715Å. The photochemical decomposition of iodide solutions has been investigated by Jortner and coworkers (1961), who observed that the quantum yield decreased with increasing *p*H up to a *p*H of 6.0. Keeping the iodide solutions at a *p*H greater than 6.0 reduces the expected quantum yield to less than 0.03.

DISCUSSION

Information reported in the literature, private communications with other workers in related research areas, and observations made during this investigation suggest definite possibilities for the plasma light source for both research and commercial applications.

Although during this investigation only about 20% of the electrical energy was converted to light, it is felt that with more efficient second generation plasma light sources this figure might well exceed 90%, with 50% of the light in the 2000 to 5000Å wavelength region.

The availability of large quantities of relatively inexpensive, high-intensity ultraviolet light is a significant advance in the technology of photochemistry. Photochemical processes which previously were not of commercial interest utilizing standard radiation sources may now merit further investigation.

Experience has shown that when high electrical power levels and light intensities are involved, small variations in design can have a profound influence on the performance of equipment. Under the extreme conditions of current, voltage, light intensity, pressure, and temperature which are inherent to the efficient operation of plasma light sources, there is no such thing as a minor equipment malfunction.

The presence of continuum radiation can frequently mean that not only the reactants but also the products will absorb radiation. This can cause either secondary reactions involving the desired products or possibly decomposition of the products. During this investigation the undesirable portion of the continuous spectra was eliminated by using selective aqueous inorganic filter solutions. This technique is generally applicable.

ACKNOWLEDGMENT

The authors express their sincere thanks to the National Science Foundation for financial support of this project.

LITERATURE CITED

Anderson, J. E., R. C. Eschenbach, and H. H. Troue, "Performance Study of a Vortex-Stabilized Arc Radiation Source," *Applied Optics*, **4**, 1435 (1965).

Cassano, A. E., P. L. Silveston and J. M. Smith, "Photochemical Reaction Engineering," *Ind. Eng. Chem.*, **59**, 18 (1967).

Irazoqui, H. A., J. Cerdà, and A. E. Cassano, "Radiation Profiles in an Empty Annular Photoreactor with a Source of Finite Spatial Dimensions," *AIChE J.*, **19**, 460 (1973).

Jortner, J., R. Levine, M. Ottolenghi, and G. Stein, "Photochemistry of the Iodide Ion in Aqueous Solution," *J. Phys. Chem.*, **65**, 1232 (1961).

Matsuura, T., and J. M. Smith, "Photodecomposition Kinetics of Formic Acid in Solution," *AIChE J.*, **16**, 1064 (1970).

Quarderer, George J., "Photochemical Chlorination of Sulfur Dioxide Utilizing a Plasma Light Source," Ph.D. thesis, University of Michigan, Ann Arbor (1967).

Papp, C. A., "Plasma and Photochemistry," *Ind. Eng. Chem.*, **55**, 48 (1963a).

———., "Plasma Technology in Chemical Processing," *Chem. Eng. Progr.*, **59**,(6), 51 (1963b).

———., "Vortex Stabilized Radiation Source," Plasmadyne Corp. Report PRE-106 (1962).

Ragonese, F. P., and J. A. Williams, "Application of Empirical Rate Expressions and Conservation Equations to Photoreactor Design," *AIChE J.*, **17**, 1352 (1971).

Regnault, V., "Note sur l'Acide Chlorosulfuric," *Ann. Chim. Phys.*, **71**, 445 (1839).

———., "Bemerkung uber die Chlorschwefelsäure," *J. Pr. Chim.*, **19**, 243 (1840).

Sandru, D., and J. M. Smith, "Photopolymerization of Acrylamide in an Annular Flow Reactor," *AIChE J.*, **19**, 558 (1973).

Villars, D. S., "The Photolysis of Potassium Nitrate," *J. Am. Chem. Soc.*, **49**, 326 (1927).